

IDENTIFICATION OF  $\mu$ s ISOMERS AMONG PRIMARY FISSION FRAGMENTS

J.W. Grüter, K. Sistemich, P. Armbruster, J. Eidens, and H. Lawin

Institut für Neutronenphysik, Kernforschungsanlage Jülich,  
Jülich, Germany

ABSTRACT

The isomeric x-rays and  $\gamma$ -rays emitted by fission products from the thermal neutron fission of  $^{235}\text{U}$  in the time window between  $1\ \mu\text{s}$  and  $80\ \mu\text{s}$  after the fission event were investigated at the gas-filled fission product separator of the research reactor FRJ-2. Isomeric transitions were detected at the fission product masses  $A = (88, 93, 96 - 100 \text{ and } 132-136)$  with about 90% of the  $\gamma$ -lines being emitted in the regions  $A = (96 - 100)$  and  $A = (132 - 136)$ . An identification of the isomeric nucleides was achieved in most cases. In the mass region  $(96 - 100)$  all identified or possible isomers have 58 or 59 neutrons. The identified isomers in the region  $A = (132 - 136)$  are  $^{134}\text{Te}$  and  $^{136}\text{Xe}$  with  $N = 82$ . The isomerism is discussed.

1. INTRODUCTION

Fission fragments are highly excited nuclei which are de-excited by neutron emission, emission of  $\gamma$ -radiation, and  $\beta$ -decays. The prompt neutrons are emitted within  $10^{-14}$  s after fission,  $\beta$ -decays occur with half-lives  $> 10^{-2}$  s. Gamma-radiation is emitted promptly as well as delayed following  $\beta$ -decays. The overwhelming part of the prompt  $\gamma$ -rays has a mean half-life of ca.  $10^{-11}$  s <sup>1,2)</sup>. But there is a considerable fraction of the prompt  $\gamma$ -radiation which is emitted from isomeric transitions with half-lives up to  $100\ \mu\text{s}$ , as was first shown for fission products from  $^{235}\text{U}$  by Maienschein et al. <sup>3)</sup>, who found an isomeric component with a half-life of  $\approx 100$  ns. In the meantime several authors have investigated such isomeric transitions. Johansson <sup>4)</sup> measured isomeric  $\gamma$ -rays of  $^{252}\text{Cf}$ -fission products in the time region  $(10 - 100)$  ns using NaJ-detectors. By measuring the kinetic energies of complementary fission products with semiconductor detectors he determined the masses of the  $\gamma$ -emitters.

He found that the isomers were concentrated into a few narrow mass regions. Popeko et al. <sup>5)</sup> investigated with a Ge(Li)-detector the isomeric  $\gamma$ -rays in the time region (10 - 100) ns after the thermal neutron fission of  $^{235}\text{U}$ . Using the same method as Johansson they determined the masses of the isomers. About 20 low energy  $\gamma$ -rays have been identified with half-lives  $< 50$  ns. Walton and coworkers <sup>6)</sup> looked for isomers among the fission products of the photofission of  $^{232}\text{Th}$ ,  $^{235}\text{U}$ ,  $^{239}\text{Pu}$  and neutron fission of  $^{235}\text{U}$ ,  $^{239}\text{Pu}$  in times  $> 2 \mu\text{s}$ . They detected the  $\gamma$ -rays with plastic detectors or NaJ-crystals. No mass assignment of the isomers has been made. The authors have identified about 10  $\gamma$ -rays with energies up to 1330 keV and half-lives up to  $54 \mu\text{s}$ . Guy <sup>9)</sup> measured the isomeric  $\gamma$ -rays of  $^{252}\text{Cf}$ -fission products with a Ge(Li)-detector and the masses of the emitters with the technique indicated before. This measurement was extended from 3 to 2000 ns after fission. The authors determined the energies, half-lives, and intensities of about 150  $\gamma$ -rays in this time region. The short-lived  $\gamma$ -rays are emitted by almost all masses that are produced with sufficient yields. The long-lived radiation, however, is confined to narrow mass regions which are similar to those in ref. <sup>4)</sup>.

Besides measurements of the  $\gamma$ -radiation there have been done experiments on x-rays emitted from isomers among the fission products due to internal conversion of the  $\gamma$ -rays. H. Hohmann <sup>7)</sup> found a delayed contribution in the x-ray spectrum from  $^{236}\text{U}$  fission, whereas Glendenin et al. <sup>8)</sup> investigated delayed x-rays from  $^{252}\text{Cf}$ . For example Watson et al. <sup>10)</sup> measured with a Si(Li)-diode the x-rays that were emitted by  $^{252}\text{Cf}$  within 93 ns. Kapoor et al. <sup>11)</sup> investigated x-rays from fission products up to  $1 \mu\text{s}$  after the thermal neutron fission of  $^{235}\text{U}$  using a NaJ-crystal. Assuming that the production of isomers is comparable for the different fissioning nuclei a comparison of the results of ref. <sup>10)</sup> and of ref. <sup>11)</sup> and of measurements of the x-rays emitted within ca.  $10^{-9}$  s after fission, see e.g. refs. <sup>8,12-14)</sup>, gives some information concerning the isomeric transitions of the fission products.

We are doing an experiment with the gas-filled fission product separator at the research reactor FRJ-2 of the Kernforschungsanlage Jülich to investigate both the  $\gamma$ -rays and the x-rays of isomers with half-lives from ca. 0.2 to  $100 \mu\text{s}$  produced by the thermal neutron fission of  $^{235}\text{U}$ .

The interest in the  $\gamma$ -radiation of fission products as a radiation emitted by very neutron rich nuclei with initially high spins and deformations has been reinforced during the recent years by the prediction of a region of stable deformations for  $Z < 50$  and  $50 < N < 82$  (4, 15-18). Isomeric transitions of the light fission products might give some information concerning this problem.

## 2. EXPERIMENTAL SET-UP

### 2.1 Separation of isotopes

The gas-filled separator providing beams of fission products from the thermal neutron fission of  $^{235}\text{U}$  has been described in some detail in refs. 19 - 21). The peculiarity of the separator is that fission products

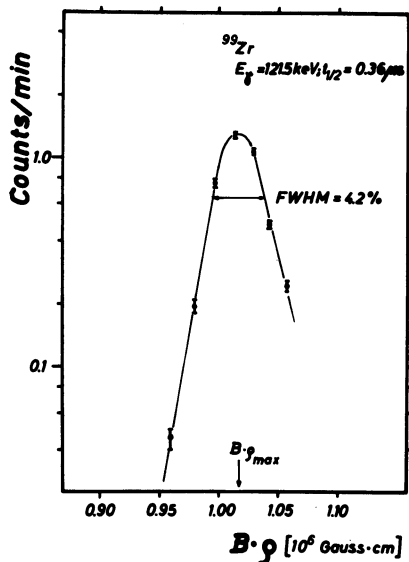


Fig. 1:  $B\cdot\phi$ -distribution of an isomeric  $\gamma$ -line

having equal nuclear charge  $Z$  and equal nuclear mass  $A$  experience the same deflection in the magnetic field of the separator, in spite of the fact that they emerge with different ionic charges and energies from the fission product source. The resolution of the separator is not sufficient to resolve single values of  $Z$  and  $A$ . At each value of the magnetic rigidity  $B\cdot\phi$  a mixture of different nucleides is obtained. A given nucleide reaches the focus of the separator within a certain range of  $B\cdot\phi$ , its distribution over  $B\cdot\phi$  being a Gaussian function. In fig. 1 an example of such a distribution is shown. The nucleide has been identified by one of the isomeric  $\gamma$ -rays that are the subject of our investigation.

The calibration of the separator has been done by measuring the intensity distributions of known  $\gamma$ -rays that follow the  $\beta$ -decays of long-lived fission products (21). The  $B\cdot\phi$ -values at which these distributions had their maxima were attributed to the masses of the  $\gamma$ -emitters. The

long-lived calibration nucleides themselves are not produced in the fission process and the subsequent prompt neutron emission, they are  $\beta$ -decay daughters of primarily produced fission products. The deflection of the calibration nucleides is determined by the mean primary charge  $Z_P(A_1)$  of the corresponding isobaric chain as the time needed for the separation is equal to the time-of-flight of the unslowed fission products through the separator which amounts to 1  $\mu$ s. Consequently the calibration curve which is shown in ref. <sup>20)</sup> may be applied, without further considerations, for the identification of long-lived secondary fission products which are deflected according to  $Z_P(A)$ .

The identification of the isomers among the primary fission products, we are interested in here, is achieved as described in the following. The distribution of an isomeric radiation over  $B \cdot \varphi$  is measured and the value  $B \cdot \varphi_{\max}$  corresponding to the maximum of this distribution is determined. To  $B \cdot \varphi_{\max}$  corresponds a mass  $A^*$  according to the calibration curve.

A mean primary charge  $Z_P^*$  may be attributed to  $A^*$  for example from the  $Z_P$ -curve of ref. <sup>22)</sup> or by interpolation between the  $Z_P$ -values of Wahl <sup>23)</sup>, both  $A^*$  and  $Z_P^*$  being usually non-integer. With these values the candidates which are possibly the emitters of the isomeric radiation can be calculated from eq. (1). This equation is obtained by expanding the three-dimensional plane  $B \cdot \varphi(Z, A)$  starting from the calibration curve in the  $Z$ -direction with  $B \cdot \varphi$  having a fixed value.

$$A - A^* = (Z_P - Z_P^*) \frac{1 - \Gamma_A}{\rho_N} - \frac{(Z_P - Z_P^*)^2}{2} \frac{d\Gamma_A/dA}{\rho_N^2} \quad (1)$$

$$\rho_N = Z_P^* / A^* \approx \text{charge density of the fissioning nucleus}$$

$$\Gamma_A = (\Delta B \cdot \varphi / B \cdot \varphi) / (\Delta A / A) = \text{mass dispersion of the separator as derived from the calibration curve.}$$

All nucleides the charge  $Z$  and mass  $A$  of which fulfil the above equation have the maximum of their  $B \cdot \varphi$ -distribution at the same value  $B \cdot \varphi_{\max}$  and may therefore be the isomer we are looking for. As the experimental values of  $A^*$ ,  $Z_P^*$ , and  $\Gamma_A$  are uncertain to some extent the mass value of a nucleide with a given  $Z$  has to fulfil eq. (1) within about  $\pm 0.7$

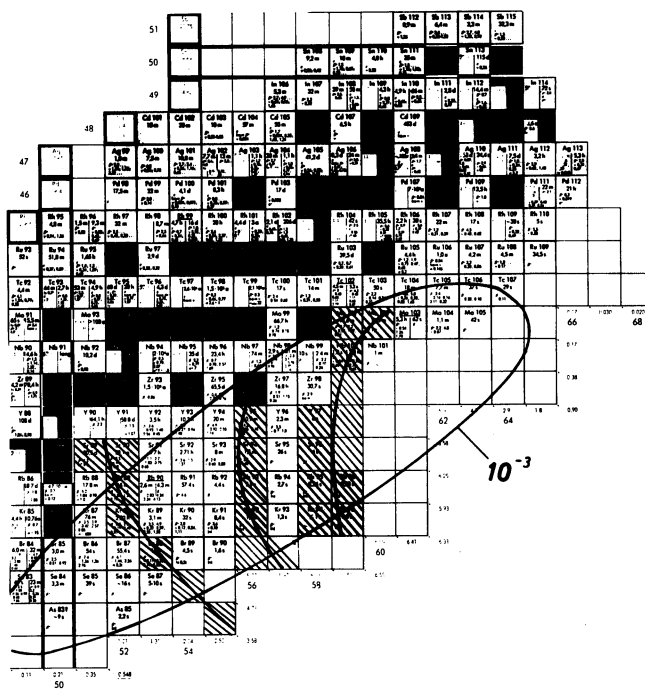


Fig. 2: Region of light fission products. The hatched bands show the nucleides focussed simultaneously in the separator.

mass units. All candidates that are determined by equation (1) lie on certain sections through the Chart of Nuclides as is demonstrated by the hatched bands in fig. 2 for light fission products. The full lines in these bands are calculated from eq. (1) without any errors of the experimental parameters. The slope of the bands are defined by  $\sqrt{A}$  which is determined by  $A^*$  and the gas-filling of the separator. The bands in fig. 2 are calculated for 6.5 torr He-gas which is the gas-filling used during the measurements in the light fission product group. It is seen that with helium the separator at certain masses of the fission products works as mass separator ( $A \approx 88$ ), at other masses it is almost an isotone separator ( $A \approx 100$ ). The region of nucleides which can be investigated with the separator is indicated in fig. 2.

If isomeric x-rays are emitted from the primary fragments, the  $B\text{-}q$ -distribution and the energy of these x-rays allow an almost unambiguous identification of the emitter. From the x-ray energy the nuclear charge  $Z$  of the emitter can be determined, and the isomer is located at the crossing point of the horizontal line for  $Z = \text{const.}$  in the  $(N, Z)$  plane, and the

section determined by eq. (1). A certain ambiguity remains if several isotopes are admitted by eq. (1).

## 2.2 Detection of isomeric radiation

The experimental arrangement installed at the focus of the separator is shown in fig. 3. The fission products are stopped by a Hostaphan-foil which is the end-window of the vacuum system. Immediately before being stopped they pass a fast transmission counter as proposed by Muga<sup>24)</sup>.

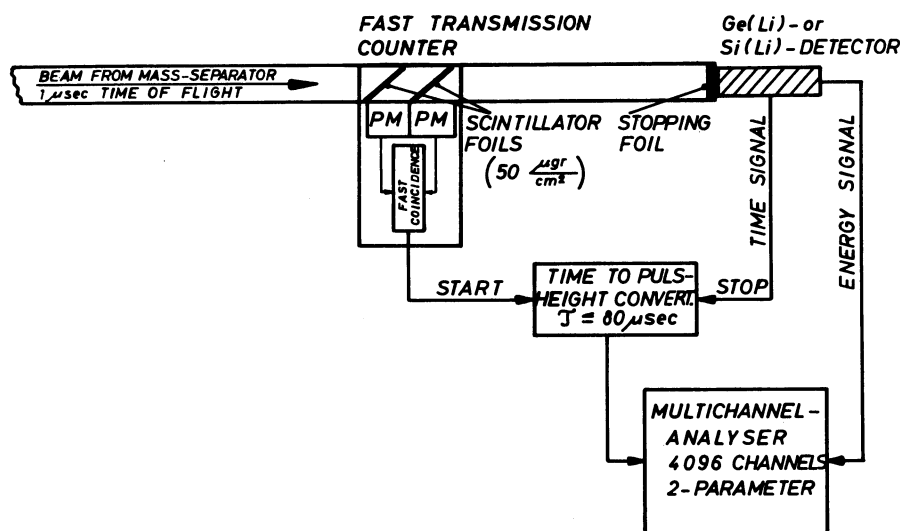


Fig. 3: The experimental arrangement at the focus of the separator

The fission products produce in a thin plastic scintillator foil of NE 102 A light which is seen by a 56 AVP-photomultiplier. By a coincidence between two such detectors we reduce the  $\gamma$ -induced background by two orders of magnitude. This transmission-counter system starts a time-to-pulse height converter (TPC) the time range of which can be varied between 0.05 and 80  $\mu$ s. The TPC is stopped by the isomeric radiation. For the measurement of isomeric  $\gamma$ -rays a Ge(Li)-diode (resolution 3.0 keV for  $^{60}\text{Co}$   $\gamma$ -rays, size 38 cm<sup>3</sup>) and of the isomeric x-rays from internal conversion of isomeric  $\gamma$ -rays a Si(Li)-detector (resolution 300 eV for  $^{57}\text{Co}$ , area = 1 cm<sup>2</sup>) are used. A 4096-channel analyser is used in the two parameter mode to store the results of the measurements i.e. the time signal of the TPC and the energies of the isomeric  $\gamma$ -rays and the energies of the isomeric x-rays, respectively. Typically the 4096 channels are divided into 32

time-channels and 128 energy-channels. The time resolution of the electronic system amounts to about 50 ns with the Si-diode and to 100 ns with the Ge-diode for low energy  $\gamma$ -rays. For high energy  $\gamma$ -rays it is considerably better. ( $\gamma$ -x)- and ( $\gamma$ - $\gamma$ )-coincidences between the detectors are possible.

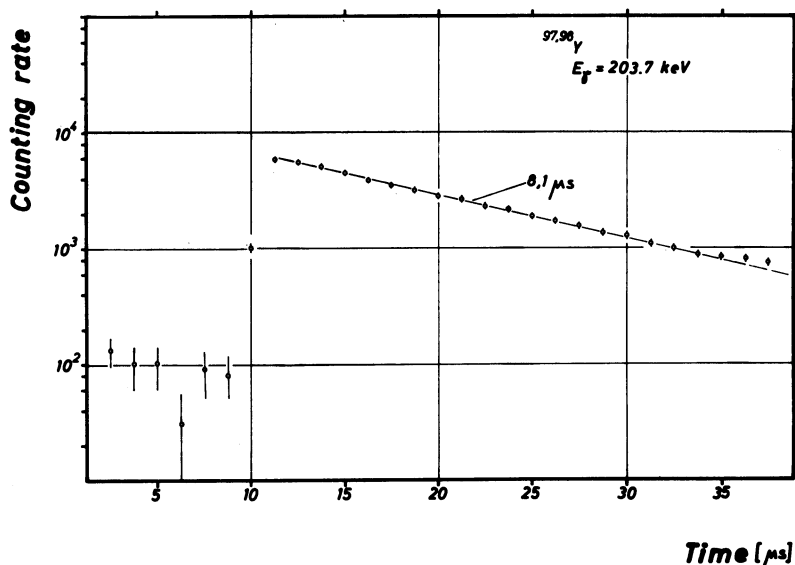


Fig. 4: A typical decay curve

Some typical experimental results are shown in figs. 1 and 4 - 6. As discussed before fig. 1 is the B- $\gamma$  distribution of the intensity of a certain isomeric  $\gamma$ -transition measured to identify the isomer. Fig 4 shows the decay curve for a certain isomeric  $\gamma$ -transition measured for a fixed value of B- $\gamma$ . Several of the  $\gamma$ -lines have a time-independent component which is produced by random coincidences between fission products and  $\gamma$ -rays with the same energy as the isomeric transition but following  $\beta$ -decays of fission products which have arrived earlier. This time-independent component is determined by delaying the stop-signals of the TPC in order to store in the first time-channels only random coincidences. The known time-independent component is then subtracted from the whole intensity measured for a certain  $\gamma$ -energy to obtain the true isomeric component. Fig. 5 shows an energy-spectrum of the Ge-diode measured for two times, i.e. just after the fission products have arrived and about

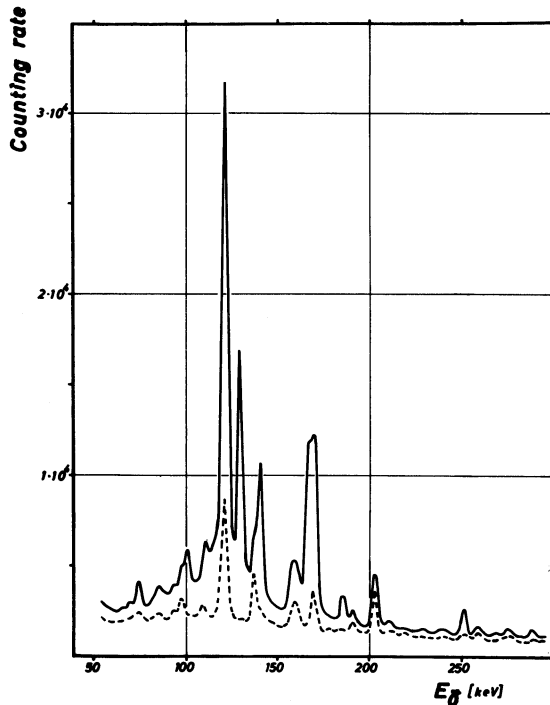


Fig. 5: Gamma-spectra measured for the mass region near  $A = 99$ , duration of the measurement = 975 min. Full line and dashed line = spectra measured after the arrival of the fission products and  $8 \mu\text{s}$  later, respectively.

$8 \mu\text{s}$  after the arrival of the fission products.  $\gamma$ -lines are seen that disappear completely within these  $8 \mu\text{s}$ . Other lines are reduced considerably or are apparently time-independent. The resolution in this picture is bad as the number of analyzer channels used is small. Fig. 6 shows the x-ray spectra just after the arrival of the fission products and random coincidence spectra.

The intensities we measure amount typically to 10/min and 1/min for isomeric  $\gamma$ -transitions of light and heavy fission products, respectively. For x-rays they are about an order of magnitude smaller. The  $(\gamma\text{-x})$ -coincidence rates are smaller than 6/h.

### 3. EXPERIMENTAL RESULTS

Our results are compiled in tables I, II, and III for light and heavy fission products, respectively. Tables I and II are divided into five parts. Part 1 gives the candidates for the isomerism calculated from eq.(1). Only the possible emitters with fission yields greater than 0.1 % are listed as we estimate the absolute intensities of our  $\gamma$ -lines to be higher than  $10^{-3}$  photons/fission. Part 2 shows the experimental facts about isomeric x-rays, part 3 gives our results of the  $\gamma$ -ray measurements. In part 4 we have added the results of Guy, ref. <sup>9)</sup>, for isomeric  $\gamma$ -transitions to compare with our  $\gamma$ -lines. In part 5 we listed the one or the few candidates which most probably emit the isomeric radiation cf. the following section. Table III contains the information about high energy isomeric  $\gamma$ -rays we found for light fission products. For these  $\gamma$ -rays the values of  $B \cdot \varphi_{\text{max}}$  have not yet been determined and thus we cannot name the possible emitters.



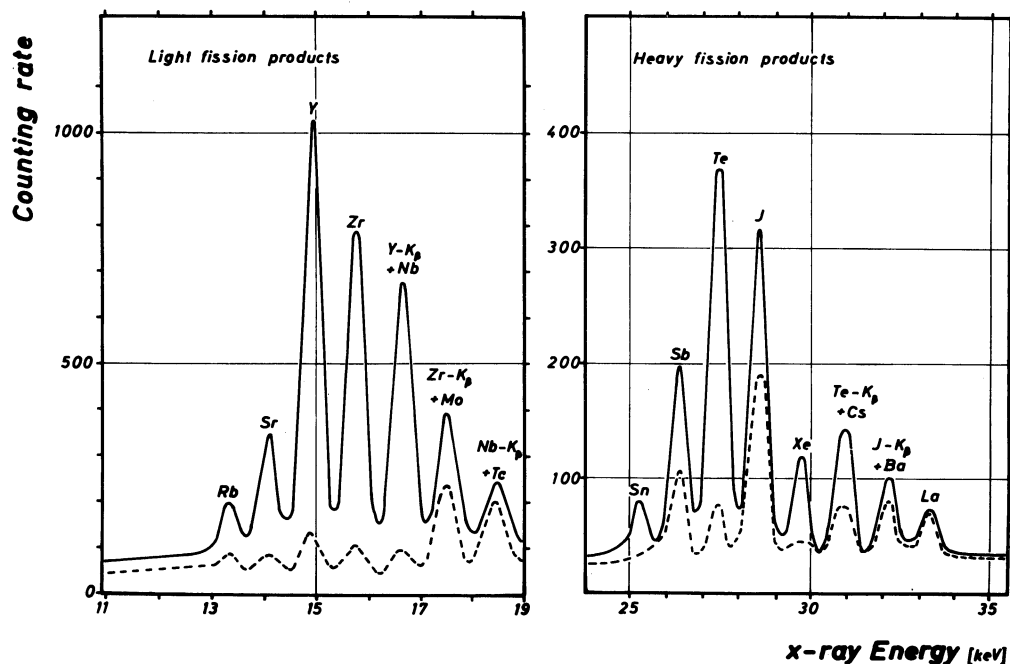


Fig. 6: x-ray spectra measured in the mass regions near  $A = 99$  and  $A = 135$  with different fission product intensities. Full lines = spectra measured just after the arrival of the fission products, dashed lines = random coincidence spectra. Duration of the measurement = 3761 min and 7528 min for light and heavy fission products, respectively.

For the light fission products we found isomeric radiation in three different mass regions as is shown by the horizontal subdivision of table I. We want to mention that the isomeric radiation of each mass group as well as all the radiation in the heavy fission product group has the same value of  $BQ_{\max}$ , a fact caused accidentally by the properties of the separator for the special gas-filling, i.e. 6.5 torr helium for light fission products and 0.5 torr nitrogen for the heavy fission product group.

We have identified some 40 isomeric  $\gamma$ -rays in the range of half-lives we investigated ( $\approx 0.3$  to  $80 \mu\text{s}$ ) and with intensities  $> 10^{-3}$  photons/fission. It is obvious from tables I and II that the candidates we have determined are concentrated in narrow fission product mass regions around  $A = 88, 93, 99$  and  $135$ . While the candidates in the regions around  $A \approx 88, 89$  emit together only three of the  $\gamma$ -lines in these tables the bulk of the  $\gamma$ -rays comes from the candidates near  $A = 99$  and  $135$ .

#### 4. DISCUSSION OF NUCLEIDE ASSIGNMENTS

As is discussed in sect. 2.1 eq. (1) admits several nucleides as candidates for the isomeric  $\gamma$ -lines detected at a certain value of  $B \cdot \varphi_{\max}$ . The uncertainties of the experimental parameters in eq. (1) which cause this ambiguity cannot be reduced essentially. The identification of the emitters of several  $\gamma$ -lines of tables I and II and the reduction of the candidates for the others is achieved by comparing our  $\gamma$ -ray results with the results of our x-ray and ( $\gamma$ -x) coincidence measurements, and with the results of the  $\gamma$ -ray measurements of other authors. The most probable emitters one gets considering all data we have are listed in part 5 of tables I and II.

##### 4.1 Light fission products

The  $\gamma$ -lines with 1110 keV and 1590 keV which are emitted by fission products with masses around 88 have the same half-lives within the experimental errors. We find the same half-life for the x-rays of Br which is the only x-ray emitter in this mass region. Therefore we conclude that Br is the emitter of the two  $\gamma$ -rays. The only Br-isotope which fulfils eq. (1) is  $^{88}\text{Br}$  and thus we assign the two  $\gamma$ -lines to  $^{88}\text{Br}$ . In ref.<sup>9)</sup> the 111.2 keV  $\gamma$ -line is assigned to the mass 89. From our results  $^{89}\text{Br}$  cannot be the emitter unless we increase the errors of the experimental parameters we insert into eq. (1) unreasonably.

We attribute the  $\gamma$ -line with  $E_{\gamma} = 257$  keV to  $^{93}\text{Rb}$  as the x-ray measurement reveals a half-life  $> 10 \mu\text{s}$  for Rb.

In the mass region near  $A = 99$  twelve  $\gamma$ -lines must be attributed to eleven possible emitters. The situation is complicated by the fact that the line  $E_{\gamma} = 169.8$  keV as well as the x-rays of Y show two different half-lives. The two half-lives might belong to different nucleides or might be caused by two isomeric states in one nucleide.

The half-lives of the long-lived component of the line with  $E_{\gamma} = 169.8$  keV as well as of the 120.1 keV and 203.7 keV lines agree within the errors with the long half-life of the Y x-rays. Thus,  $^{97}\text{Y}$  or  $^{98}\text{Y}$  is most probably the emitter of this  $8 \mu\text{s}$ -radiation, in agreement with the mass assignment of ref.<sup>9)</sup> for the 204.0 keV line. A first ( $\gamma$ -x)-coincidence measurement gives coincidences between these lines and the x-rays of Y.

The assignment of the short-lived  $\gamma$ -transitions in this mass region is complicated by the fact that the short half-lives of the  $\gamma$ -rays as well as of the x-rays are very similar. Thus, the comparison between the half-lives of  $\gamma$ -rays and x-rays provides no unique identification of the nuclear charge of the isomer emitting a certain  $\gamma$ -line. The  $\gamma$ -lines with  $E_\gamma = 101.0, 110.7, 130.0, 158.9, \text{ and } 185.3$  keV are in coincidence with the x-rays of Y. They are grouped in table I according to their half-lives including the short-lived component of the 169.8 keV-line. The half-lives of these lines agree within the errors, except the line with  $E_\gamma = 130.0$  keV. We conclude that these lines are emitted by  $^{98}\text{Y}$  as the mass assignment of ref. <sup>9)</sup> for two of them is  $A = 98$ . The half-life of the 130.0 keV-line is considerably smaller. If we assume a third isomeric state in Y; the half-life of  $0.6 \mu\text{s}$  of the x-rays of Y may be composed of the half-life of the 130.0 keV-line and of the half-lives of the lines assigned to  $^{98}\text{Y}$ . According to ref. <sup>9)</sup> the mass of the emitter of the 130.0 keV-line is 99 or 100 giving with eq. (1) the candidates  $^{99}\text{Zr}$  and  $^{100}\text{Nb}$ . This mass assignment does not agree with the result of our ( $\gamma$ -x)-coincidence measurement and the assumption of a third isomeric state in Y isotopes.

The 140.5 keV-line is in coincidence with the x-rays of Rb. The assignment of this  $\gamma$ -line to  $^{96}\text{Rb}$  is in agreement with the half-life of the x-rays of Rb and with the mass determination of ref. <sup>9)</sup>. The 167.2 keV-line is also attributed to  $^{96}\text{Rb}$  as its half-life and the mass assignment of ref. <sup>9)</sup> agree with the values of the 140.5 keV-line.

The 121.5 keV-line is in coincidence with the x-rays of Zr. Thus,  $^{99}\text{Zr}$  is the emitter in agreement with the x-ray half-life of Zr and with the mass of ref. <sup>9)</sup>. As we see the 121.5 keV-line in coincidence with the x-rays of Zr there must be another transition in Zr, which causes the corresponding x-ray emission and which we do not see as a  $\gamma$ -line.

#### 4.2 Heavy fission products

The relations are more transparent in the heavy fission product group. The  $\gamma$ -lines in table II are grouped according to the four half-lives we found. In ref. <sup>9)</sup> the lines with  $E_\gamma \approx 115, 297, 1280$  keV are attributed to  $^{134}\text{Te}$ . It is assumed that they are emitted in a cascade with the 115 keV and the 1280 keV line as the highest and the lowest transition, respecti-

vely. The same cascade has been detected by Ahrens et al. <sup>25)</sup> following the  $\beta$ -decay  $^{134}\text{Sb} \rightarrow ^{134}\text{Te}$ . Our results agree with this assignment.

The  $\gamma$ -lines with  $E_\gamma \approx 197, 381$  and  $1313$  keV and with half-lives of about  $3 \mu\text{s}$  are assigned in ref. <sup>9)</sup> to  $^{136}_{54}\text{Xe}$ . This assignment was supported by the  $^{136}\text{Xe} (p, p') ^{136}\text{Xe}$  measurement of Moore et al. <sup>26)</sup> who found levels in  $^{136}\text{Xe}$  in which the  $\gamma$ -rays fit as a cascade going to the ground-state. This attribution is in agreement with our half-life for the x-rays of Xe. Walton et al. <sup>6)</sup> found  $\gamma$ -lines with  $E_\gamma = 205, 390, 1330$  and the half-life  $3.4 \pm 0.4 \mu\text{s}$  in their measurement with a NaJ-crystal. The  $\gamma$ -lines were also seen following the  $\beta$ -decay of 48 s-isomer of  $^{136}\text{J}$  with high spin (27-30). While Lundan et al. <sup>28)</sup> proposed a cascade 198 keV - 382 keV - 1320 keV - 1313.2 keV going to the ground-state, Carraz et al. <sup>29)</sup> and Monnard et al. <sup>30)</sup> found a cascade 197.5 keV - 381.5 keV - 1313.3 keV going to the ground state.

The 391 keV  $\gamma$ -line is attributed to  $^{134-136}\text{J}$  according to the half-life. Not identified is the emitter of the two remaining  $\gamma$ -lines in table II with  $E_\gamma = 324$  keV and 1181 keV and a half-life of about  $0.65 \mu\text{s}$ . The half-lives of the x-rays of Sn, Sb, Te agree with this  $\gamma$ -half-life. According to the mass determination of ref. <sup>9)</sup> this radiation is emitted from fission products with  $A = 134, 135$ . Thus  $^{134,135}\text{Sb}$  and  $^{134,135}\text{Te}$  are the most probable emitters.

## 5. CONCLUSIONS

A comparison of the detected  $\gamma$ -lines from this measurement and from ref. <sup>9)</sup> shows good agreement for the  $\gamma$ -energies and for the half-lives shorter than  $1 \mu\text{s}$ . Intensities for the different fissioning systems have not been compared. The lines with low intensities of table III have not been listed in ref. <sup>9)</sup>.

A comparison between the isomeric x-ray yields of ref. <sup>10)</sup> and ref. <sup>11)</sup> shows that for times  $> 0.1 \mu\text{s}$  x-rays may be expected from Rb, Sr, Y, Nb, Mo, Tc and Sb, Te, J, Xe. X-rays from these elements have been found, except from Mo, Tc. The time-dependent components of the x-rays with energies corresponding to Mo and Tc in fig. 6 are caused by the  $K_\beta$ -radiation of nuclei with lower Z-values. Additionally we found a strong emission of x-rays at Zr.

As may be seen from part 5 of tables I and II the isomers we found are concentrated, except of two single isomers  $^{88}\text{Br}$  and  $^{93}\text{Rb}$ , in two mass regions,  $A = (96 - 100)$  and  $A = (132 - 136)$ . This fact is in agreement with the results of ref. 9) for  $^{252}\text{Cf}$ , where an intense long-lived contribution to the isomeric  $\gamma$ -radiation near these masses has been detected. Moreover, Johansson 4) observed an intense delayed  $\gamma$ -radiation for  $A \approx 96$  and  $A = (130 - 135)$ .

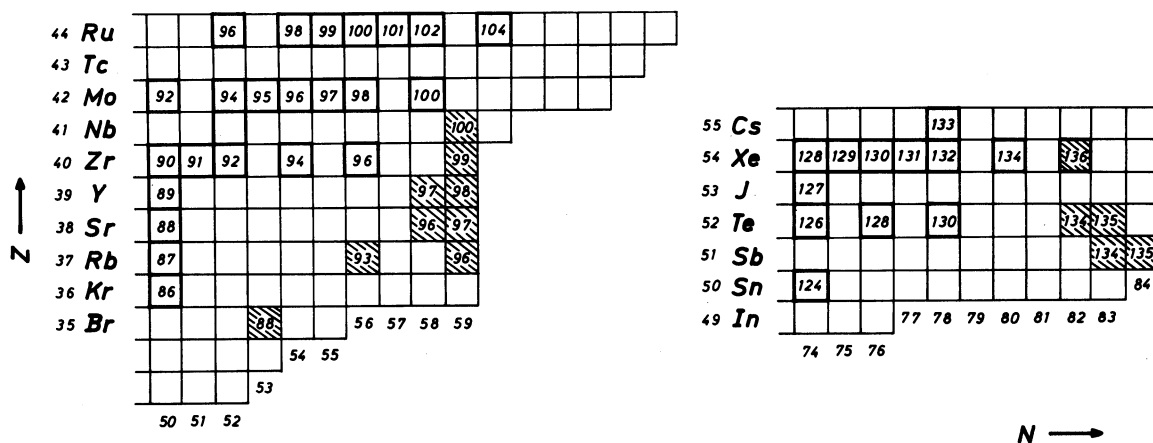


Fig. 7 : The most probable emitters (hatched) inserted in the Chart of Nuclides. The stable nuclides are shown for orientation.

In the heavy fission product region isomers are found with  $N = (82 \pm 1)$ . There are (g,g)-nuclei among the emitters, as  $^{134}\text{Te}$  and  $^{136}\text{Xe}$ . The  $\gamma$ -lines emitted as isomeric radiation have been found after  $\beta$ -decays 25, 27-30) and some of them promptly within a few ns after fission 31). The x-ray spectrum emitted following  $\beta$ -decay (dashed line in fig. 6) has a similar structure as the isomeric x-ray spectrum. The isomers from even-Z-nuclei only seem to be populated more intensely primarily than after  $\beta$ -decay. The isomeric states of  $^{136}\text{Xe}$  and  $^{134}\text{Te}$  are located at 1891 keV and 1692 keV above the ground state, respectively. These states fit well into the systematics of isomeric states of  $N = 82$  nuclei 29). A low lying two-quasi-particle neutron state  $(g_{7/2})^2$  with high spin  $I = (5 - 7)$  may have enhanced life times in the nuclei of low level density near the closed shells  $N = 82$  32). The isomerism found is thus explained as spin isomerism of states which are populated both primarily and after  $\beta$ -decay. Isomers with odd neutron or proton numbers may be understood as long-lived three-quasi-

particle states of these nucleides which should be found at lower energies.

Fig. 7 reveals a striking observation in the mass region  $A = (96-100)$ . All nucleides we have identified or proposed as candidates have the neutron number  $N = 58$  or  $59$ , i.e. the bulk of the isomeric  $\gamma$ -rays with half-lives larger than  $0.3 \mu\text{s}$  among the light fission products is emitted from nucleides with  $N = (58-59)$ . No even  $A$ , even  $Z$  nucleides are found among the emitters, except  $^{96}\text{Sr}$  as possible x-ray emitter. The isomeric  $\gamma$ -lines have not been observed until now among the  $\gamma$ -lines following  $\beta$ -decays of the fission products. The dashed x-ray spectra shown in fig. 6 is mainly determined by x-rays following  $\beta$ -decays of short-lived fission products. The x-ray yields following  $\beta$ -decays show no similarities with the yield we found for isomeric x-rays pointing again to the fact that the isomeric  $\gamma$ -transitions with their characteristic x-ray-yields are only found among the primary fission products. From the energies and yields of the primary  $\gamma$ -quanta we estimate that the isomeric states in the region of  $N = (58-59)$  are about  $(300 - 400)$  keV above the ground state.

We cannot offer a definitive explanation of the isomerism among light fission products. An accidental pile-up of spin isomers, although not very probable, cannot be excluded. We want to point out an unproved hypothesis to explain the isomerism. According to calculations of Arseniev et al. <sup>17)</sup>  $N = (58-60)$  is a transition region to a new region of deformed nuclei. Nuclei with  $N \approx 59$  should have a stable oblate deformation with an energy excess of about 2 MeV compared to a spherical shape. Excited states of these nuclei may have prolate shapes as has been shown by Arseniev et al. <sup>33)</sup> for nuclei in the mass region  $Z > 50$  and  $N < 82$ . These states may be found at low energies, if the difference between the deformation energies of prolate and oblate shapes is small. They may be observed as low lying one-quasi-particle states with lifetimes enhanced due to large values of  $\Delta K$ . If these states are the explanation for the isomerism at  $N = (58-59)$ , our measurements tell that this shape isomerism is restricted to the transition region and is not found with half-lives in the  $\mu\text{s}$  range within the region of stable deformations for  $N > 60$ .<sup>\*</sup> It should be pointed out that a further transition region exists for  $Z = (45-46)$  in the mass range  $A = (110-115)$ .

---

\* The confinement of the isomerism to the transition region may be explained if a co-existence of deformed and spherical states is postulated, as has been found for Ir-nuclei<sup>34)</sup>.

In this region, too, isomers are located, as has been shown in ref. <sup>4),9)</sup> in experiments with <sup>252</sup>Cf fission products. More extensive calculations and new measurements in the transition region may help to prove or disprove the hypothesis of the new proposed shape isomerism.

#### REFERENCES

- 1) S.A.E. Johansson, Nuclear Phys. 60, 387 (1964).
- 2) H. Labus, Kernforschungsanlage Jülich, Report JÜL-643-FN
- 3) F.C. Maienschein, R.W. Peele, W. Zobel, and T.A. Love, Proceedings of the Second Int. Conf. on the Peaceful Uses of Atomic Energy 15 (Geneva, 1958) paper P/670, p. 366.
- 4) S.A.E. Johansson, Nuclear Phys. 64, 147 (1965).
- 5) L.A. Popeko, G.V. Valskii, D.M. Kaminkev, and G.A. Petrov, J. Nucl. Energy Parts A/B, 20, 811 (1966).
- 6) R.B. Walton, R.E. Sund, E. Haddad, and J.C. Young, Phys. Rev. 134, B 824 (1964).  
R.E. Sund and R.B. Walton, Phys. Rev. 146, 824 (1966).  
R.B. Walton and R.E. Sund, Phys. Rev. 178, 1894 (1969).
- 7) H. Hohmann, Z. Physik 172, 143 (1963).
- 8) L.E. Glendenin, J.P. Unik, and H.C. Griffin, Proc. of the IAEA-Symposium on Physics and Chemistry of Fission, Salzburg 1965, paper SM - 60/31.
- 9) F.W. Guy. UCRL - 50810, and  
W. John, F.W. Guy, and J.J. Wesolowski, UCRL 72 501 (to be published).
- 10) R.L. Watson, R.H. Bowman and S.G. Thompson, Phys. Rev. 162, 1169 (1967).
- 11) S.S. Kapoor, V.S. Ramamurthy, and R. Zaghoul, Phys. Rev. 177, 1776 (1969).
- 12) S.S. Kapoor, H.R. Bowman, and S.G. Thompson, Phys. Rev. 140, B 1310 (1965).
- 13) R.A. Atneosen, T.D. Thomas, W.M. Gibson, and M.L. Perlman, Phys. Rev. 148, 1206 (1966).
- 14) R.L. Watson, J.B. Wilhelmy, R.C. Jared, C. Ruge, H.R. Bowman, S.G. Thompson, and J.O. Rasmussen, Nucl. Physics A 141, 449 (1970).
- 15) R.K. Sheline, Revs. Modern Phys., 32, 1 (1960).
- 16) S.A.E. Johansson, Ark. Fys. 36, 599 (1967).

- 17) D.A. Arseniev, A. Sobiczewski, and V.G. Soloviev, Nucl. Physics A 139, 269 (1969).
- 18) S.G. Nilsson, "Results of equilibrium calculations in the fission product mass region", contribution to this conference.
- 19) P. Armbruster, J. Eidens, and E. Roeckl, Ark. Fys. 36, 293 (1967).
- 20) E. Roeckl, J. Eidens, and P. Armbruster, Z. Physik 220, 101 (1969).
- 21) J. Eidens, E. Roeckl, and P. Armbruster, Nucl. Physics A 141, 289 (1970)
- 22) K. Sistemich, P. Armbruster, J. Eidens, and E. Roeckl, Nucl Physics A 139, 289 (1969).
- 23) A.C. Wahl, A.E. Norris, R.A. Rouse, and J.C. Williams, Proc. of the Second IAEA Symposium on Physics and Chemistry of Fission, Vienna 1969, p. 813. Results of the calculation described there are submitted as private communication of A.C. Wahl.
- 24) M.L. Muga, Nuclear Chemistry Progress Report, University of Florida, ORO-2843 -12, (1967), ORO - 2843 - 13 (1968).  
M.L. Muga, D.J. Burnsed, W.E. Steeger, and H.E. Taylor, Nucl. Instr. and Meth. 83, 135 (1970).
- 25) Private communication by H. Ahrens, Institut für Anorganische Chemie und Kernchemie, Universität Mainz, Germany
- 26) P.A. Moore, P.J. Riley, C.M. Jones, M.O. Mancusi, and J.L. Forster, Jr., Phys. Rev. 1C, 1100 (1970).
- 27) N.R. Johnson and G.D.O Kelley, Phys. Rev. 114, 279 (1959).
- 28) A. Lundan and A. Suvola, Ann. Acad. Sci. Fennicae, A 6 (1968).
- 29) L.C. Carraz, J. Blachot, E. Monnard, and A. Moussa, private communication, submitted to Nuclear Physics.
- 30) E. Monnard, J. Blachot, L.C. Carraz, and A. Moussa, "Short-lived isomers of  $^{136}\text{J}$  and  $^{138}\text{Cs}$  decaying via metastable states of  $^{136}\text{Xe}$  and  $^{138}\text{Ba}$ ", contribution to this conference.
- 31) F. Horsch, thesis, Universität Karlsruhe.
- 32) L.S. Kisslinger and R.A. Sorenson, Mat. Fys. Medd. Dan. Vid. Selsk. 32, No. 9 (1960).
- 33) D.A. Arseniev, A. Sobiczewski, and V.G. Soloviev, Nucl. Physics A 126, 15 (1969).
- 34) A. Baecklin, G. Hedin, S.G. Malmskog, and V. Berg, "Nuclear co-existence in odd-mass Ir-nuclei", contribution to this conference.



nuclide assignment by separator from eq.(1)	isomeric x-rays			isomeric $\gamma$ -rays			most probable isomers		
	this work		ref. 9)		mass				
	element	$t_{1/2}$ [ $\mu$ s]	rel. yield	$E_\gamma$ [keV]		$t_{1/2}$ [ $\mu$ s]			
$^{88}\text{Se}$ ; $^{88}\text{Br}$ ; $^{88,89}\text{Kr}$ ; $^{89}\text{Rb}$							$^{88}\text{Br}$		
	Br	$6.8 \pm 1.0$	-	$111.0 \pm 0.5$ 159.0	$6.2 \pm 0.6$ $6.5 \pm 0.6$	45 57		111.2	3.0*
$^{91}\text{Br}$ ; $^{92}\text{Kr}$ ; $^{93}\text{Rb}$ ; $^{93,94}\text{Sr}$ ; $^{95}\text{Y}$ ; $^{96}\text{Zr}$							$^{93}\text{Rb}$		
	Rb	$>10$	-	257.0	$57 \pm 15$	-		-	-
$^{94}\text{Kr}$ ; $^{95,96}\text{Rb}$ ; $^{96,97}\text{Sr}$ ; $^{97,98}\text{Y}$ ; $^{99}\text{Zr}$ ; $^{100}\text{Nb}$ ; $^{101,102}\text{Mo}$	Rb	$0.51 \pm 0.18$	38	140.5 167.2	$0.48 \pm 0.1$ $0.50 \pm 0.1$	41 40	140.9 167.1	0.36 0.24	$96 \pm 1, -0$
	Sr	$0.47 \pm 0.08$	105	-	-	-	-	-	$96, 97 \text{ Sr}$
	Y	$0.6 \pm 0.1$ $8.2 \pm 0.9$	248 100	130.0	$0.44 \pm 0.1$	72	129.8	0.34	$99 \pm 1, -0$
				101.0	$0.84 \pm 0.15$	15	100.7	0.53	$98 \pm 0, -1$
				110.7	$0.90 \pm 0.15$	7	111.0	0.76	$98 \pm 0$
			158.9	$0.75 \pm 0.2$	9	158.0	1.50	$97 \pm 1$	
			169.8	$0.62 \pm 0.15$	35	170.5	1.1	$98 \pm 0$	
			185.3	$0.85 \pm 0.1$	8	186.4	0.65	$98 \pm 1$	
			120.1	$7.9 \pm 0.3$	100	-	-	-	$97.98 \text{ Y}$
			169.8	$8.1 \pm 0.3$	64	-	-	-	-
			203.7	$8.1 \pm 0.3$	69	204.0	3.0*	$98 \pm 1$	-
Zr	$0.32 \pm 0.08$	550*	121.4	$0.36 \pm 0.05$	110	121.4	0.36	$99 \pm 1, -0$	$99 \text{ Zr}$
Nb	$0.32 \pm 0.08$	345*	-	-	-	-	-	-	$^{100}\text{Nb}$

\* estimated value

Table II : Isomeric x- and  $\gamma$ -rays measured for heavy fission products

nuclide assignment by separator from eq.(1)	isomeric x-rays			this work				isomeric $\gamma$ -rays (ref.9)			most probable isomers
	element	$t_{1/2}$ [ $\mu$ s]	rel. yield	$E_{\gamma} + 0.5$ [keV]	$t_{1/2}$ [ $\mu$ s]	rel. yield	$E_{\gamma}$ [keV]	$t_{1/2}$ [ $\mu$ s]	mass		
$^{132, 133}\text{Sn}$ $^{134, 135}\text{Sb}$ $^{134, 135}\text{Te}$	Sn	$0.53 \pm 0.2$	2.3	-	-	-	-	-	-	-	$^{132, 133}\text{Sn}$
	Sb	$0.58 \pm 0.12$	4.4	324	$0.57 \pm 0.05$	6.6	324.5	0.57	$135 \pm 0$	$134, 135$	$^{134, 135}\text{Sb}$
				1181	$0.59 \pm 0.05$	11	1181.0	0.57	$135 \pm 0, -1$		
Te	$0.18 \pm 0.1$	100	115 297 1280	$0.19 \pm 0.05$ $0.22 \pm 0.05$ $0.18 \pm 0.05$	44 64 100	115.0 296.9 1279.8	0.162 0.164 0.164	$134 \pm 0$	$^{134}\text{Te}$		
$^{134-136}\text{J}$ $^{137}\text{Cs}$	J	$0.97 \pm 0.15$	5.4	391	$1.4 \pm 0.3$	0.7	-	-	-	-	$^{134-136}\text{J}$
	Xe	$1.8 \pm 1.2$	2.8	197 381 1313	$3.3 \pm 0.3$ $3.2 \pm 0.3$ $3.0 \pm 0.3$	6.3 4.1 4.2	197.3 380.7 1313.3	2.8 3.4 3.0	$137 \pm 0$ $137 \pm 1$ $137 \pm 2, -1$	$^{136}\text{Xe}$	

Table III : Isomeric  $\gamma$ -rays of the light group without detailed nuclide assignment

$E_{\gamma}$ [keV]	229	$240.5$	252	275	308	325	345	432	522	661	772
$t_{1/2}$ [ $\mu$ s]	$< 1$	$20 \pm 5$	$0.44 \pm 0.05$	$25 \pm 5$	$< 1$	$10 \pm 2$	$< 1$	$2 \pm 1$	$< 1$	$< 1$	$\approx 1$
rel. yield*	1.3	3.7	4.1	9.8	0.8	10	2.3	3.3	5.2	5.4	4.2

\*related to 100 in table I